

Microplate Modeling under Coupled Structural-Fluidic-Electrostatic Forces

Mohammad I. Younis and Ali H. Nayfeh

Department of Engineering Science and Mechanics, MC 0219, Virginia Polytechnic Institute and State University, Blacksburg, Virginia 24061, USA, anayfeh@vt.edu

ABSTRACT

We present a model for the dynamic behavior of microplates under the coupled effects of squeeze-film damping, electrostatic actuation, and mechanical forces. The model simulates the dynamics of microplates and predicts their quality factors under a wide range of gas pressures and applied electrostatic forces up to the pull-in instability. The model utilizes the nonlinear Euler-Bernoulli beam equation, the linearized dynamic von-Kármán plate equations, and the linearized compressible Reynolds equation. The static deflection of the microplate is calculated using the beam model. Perturbation techniques are used to derive analytical expressions for the pressure distribution in terms of the plate mode shapes around the deflected position. The static deflection and the analytical expressions are substituted into the plate equations, which are solved using a finite-element method.

Keywords: Microplates, squeeze-film damping, electrostatic forces, quality factors.

1 INTRODUCTION

MEMS devices widely employ a parallel-plate capacitor, in which one plate is actuated electrically and its motion is detected by capacitive changes. To increase the efficiency of actuation and the sensitivity of detection, the distance between the capacitor plates is minimized and the sizes of the plates are maximized. Under such circumstances, squeeze-film damping becomes increasingly pronounced.

We present a model for microplates under the effect of squeeze film damping, electrostatic actuation, and mechanical forces. The majority of the literature is dedicated to rigid structures. Few papers treat flexible structures. However, they use approximations in the structural problem while solving the fluidic problem [1] and vice versa, despite the fact that both problems are coupled. Other models require many iterations between different energy-domain CAD solvers, making the simulation process cumbersome. Further, no model has been presented to calculate the plate mode shapes, their natural frequencies, and quality factors, while sweeping the DC voltage up to the pull-in instability. Such problems

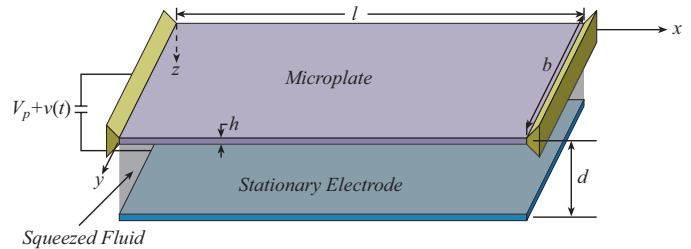


Figure 1: Electrically actuated microplate under the effect of squeeze-film damping.

are of significant importance for many MEMS applications, such as electrostatic projection displays.

In a previous work [2], we presented a beam model that simulates the behavior of electrically actuated microstructures up to the pull-in instability. However, the model does not account for squeeze-film damping. In [3], we presented a model utilizing a linearized plate equation coupled with the compressible Reynolds equation to simulate the dynamic behavior of microstructures under the effect of squeeze-film damping and small DC loading. However, the model does not apply for plates actuated by large electrostatic forces or exhibiting large deflections.

In this work, we utilize the beam model in [2] to simulate the static behavior of the microplate under the effect of electrostatic forces. We derive from the compressible Reynolds equation analytical expressions for the pressure distribution in terms of the plate mode shapes around the deflected position, and hence eliminate the pressure as a variable in the solution procedure. We substitute the static deflection and the analytical expression of the pressure in the dynamic von-Kármán plate equations, linearized around the deflected position. We then solve the resulting equations using a finite-element method.

2 PROBLEM FORMULATION

We consider a microplate, Figure 1, actuated by an electric load composed of a DC component V_p and an AC component $v_e(t)$ and subject to a net pressure force $\bar{P}(x, y, t)$ per unit area due to squeeze-film damping. The electrostatic force varies along the length of the

plate and is constant across its width. The electrostatic force deflects the microplate to a new equilibrium position. We assume that the pressure around the deflected plate is redistributed such that $\bar{P} = 0$. Because of the symmetric nature of the electrostatic forces and the boundary conditions, we use the nonlinear Euler-Bernoulli beam model in [2] to calculate the static deflection w_s of the plate. We use the dynamic version of the von-Kármán plate equations to represent the microplate motion.

To derive the linear damped eigenvalue problem describing the free vibration of the microplate, we linearize the von-Kármán plate equations around w_s , drop the forcing term $v_e(t)$, and obtain

$$\begin{aligned} \nabla^4 W_n - N W_{n,xx} - \alpha_1 U_{n,x} w_{s,xx} - \alpha_2 W_{n,xx} w_{s,x}^2 \\ - \alpha_3 V_{n,y} w_{s,xx} - \alpha_4 W_{n,yy} w_{s,x}^2 - \omega_n^2 W_n - \alpha_5 \frac{V_p^2 W_n}{(1-w_s)^3} \\ + P_{non} P_n = 0 \end{aligned} \quad (1)$$

$$\begin{aligned} U_{n,xx} + \alpha_6 W_{n,x} w_{s,xx} + \alpha_6 w_{s,x} W_{n,xx} + \nu V_{n,xy} \\ + \frac{1}{2}(1-\nu)(U_{n,yy} + V_{n,xy} + \alpha_6 w_{s,x} W_{n,yy}) = 0 \end{aligned} \quad (2)$$

$$\begin{aligned} V_{n,yy} + \nu U_{n,xy} + \nu \alpha_6 w_{s,x} W_{n,xy} + \frac{1}{2}(1-\nu)(U_{n,xy} \\ + V_{n,xx} + \alpha_6 w_{s,x} W_{n,xy} + \alpha_6 W_{n,y} w_{s,xx}) = 0 \end{aligned} \quad (3)$$

where $W_n(x, y)$, $V_n(x, y)$, and $U_n(x, y)$ are the n th transverse, lateral, and longitudinal complex mode shapes of the plate, respectively, at the nondimensional positions x and y , $P_n(x, y)$ is the corresponding n th pressure mode shape, and ω_n is the n th complex nondimensional eigenvalue. The nondimensional parameters appearing in equations (1-3) are

$$\begin{aligned} N = \frac{N_1 \ell^2}{D}, \quad P_{non} = \frac{P_a \ell^4}{dD}, \quad T^2 = \frac{\rho h \ell^4}{D} \\ \alpha_1 = \frac{\ell d d_3}{D}, \quad \alpha_2 = \frac{d_3 d^2}{2D}, \quad \alpha_3 = \frac{\nu \ell d}{D} \\ \alpha_4 = \frac{\nu d_3 d^2}{2D}, \quad \alpha_5 = \frac{\epsilon \ell^4}{D d^3}, \quad \alpha_6 = \frac{d}{\ell} \end{aligned} \quad (4)$$

where d is the initial gap width, $D = \frac{Eh^3}{12(1-\nu^2)}$ is the plate flexural rigidity, h is the microplate thickness, E is Young's modulus, ν is Poisson's ratio, \hat{N}_1 is the axial force per unit length in the x direction, ϵ is the dielectric constant of the gap medium of the airgap, ρ is mass density of the plate, and P_a is the static pressure in the airgap. The symbol ∇^4 denotes the nondimensional biharmonic operator ($\nabla^4 = W_{n,xxxx} + 2W_{n,xyyy} + W_{n,yyyy}$), where a comma denotes partial differentiation with respect to the corresponding coordinate. The parameter d_3 is defined as

$$d_3 = \frac{Eh}{1-\nu^2} \quad (5)$$

The parameter ω_n is related to the dimensional complex frequency ω by $\omega = \omega_n/T$. The structural boundary conditions for the case in Figure 1 are

At $y = 0$ and $y = b/\ell$

$$V_{n,y} + \nu \alpha_6 U_{n,x} + \nu w_{s,x} W_{n,x} = 0 \quad (6)$$

$$U_{n,y} + V_{n,x} + \alpha_6 w_{s,x} W_{n,y} = 0 \quad (7)$$

$$W_{n,yy} + \nu W_{n,xx} = 0 \quad (8)$$

$$W_{n,yyy} + (2-\nu)W_{n,xy} = 0 \quad (9)$$

Clamped edges at $x = 0$ and $x = 1$

$$U_n = 0 \quad (10)$$

$$V_n = 0 \quad (11)$$

$$W_n = 0 \quad (12)$$

$$W_{n,x} = 0 \quad (13)$$

We assume small variations of pressure around P_a and write the following nondimensional Reynolds equation, linearized around w_s and P_a , governing the pressure distribution underneath the microplate:

$$\begin{aligned} \frac{\partial}{\partial x} [(1-w_s)^3 P_{n,x}] + \frac{\partial}{\partial y} [(1-w_s)^3 P_{n,y}] \\ = i\sigma\omega_n [(1-w_s)P_n - W_n] \end{aligned} \quad (14)$$

where $\sigma = \frac{12\eta_{eff}\ell^2}{d^2 P_a T}$ is the squeeze number and η_{eff} is the effective viscosity [4] of the fluid in the gap. The pressure boundary conditions for the case in Figure 1 are zero-flux pressure at the clamped edges of the plate and trivial pressure at the open edges; that is,

$$P_{n,x}(0, y) = P_{n,x}(1, y) = 0 \quad (15)$$

$$P_n(x, 0) = P_n(x, b/\ell) = 0 \quad (16)$$

Because typically $\omega_n \sigma \gg 1$, the boundary-value problem represented by equations (14-16) is a singular-perturbation problem [5]. In this problem, the pressure changes sharply near the free edges. We use the method of matched asymptotic expansions [5] to derive a uniform approximation to the solution of equations (14-16), which yields

$$\begin{aligned} P_n(x, y) = \frac{1}{1-w_s} \left[W_n(x, y) - W_n(x, b/\ell) e^{\frac{-1+i}{\sqrt{2}} \frac{b/\ell-y}{\sqrt{\epsilon(1-w_s)}}} \right. \\ \left. - W_n(x, 0) e^{\frac{-1+i}{\sqrt{2}} \frac{y}{\sqrt{\epsilon(1-w_s)}}} \right] \end{aligned} \quad (17)$$

where $\epsilon = 1/(\omega_n \sigma)$. Equation (17) gives an approximate analytical expression for the n th complex pressure mode shape in terms of the n th complex plate mode shape and eigenvalue.

3 RESULTS

We substitute equation (17) into equation (1) and obtain an equation, which along with equations (2,3,6-13), represent a linear distributed-parameter system for the dynamic behavior of the microplate under the coupled effect of squeeze-film damping, structural forces, and electrostatic forces. We solve this system for the n th complex mode shape and eigenvalue using a finite-element method. The real part of the complex eigenvalue yields frequency of the microplate, whereas the ratio between its real and twice the imaginary part yields the quality factor.

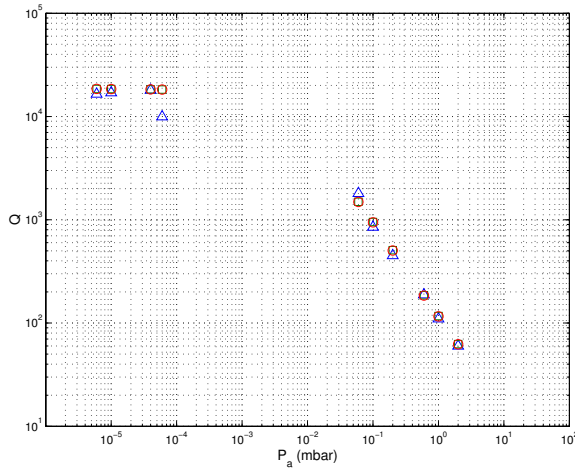
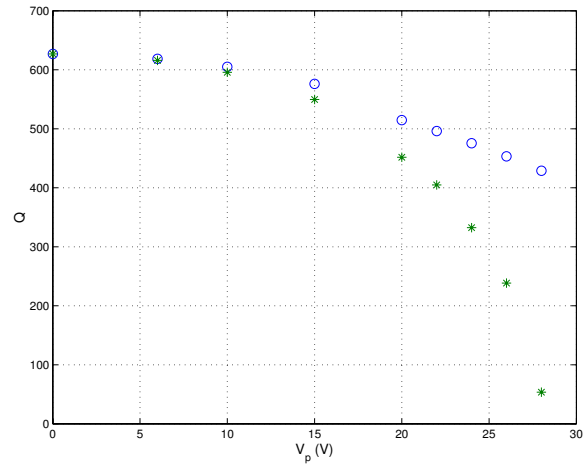


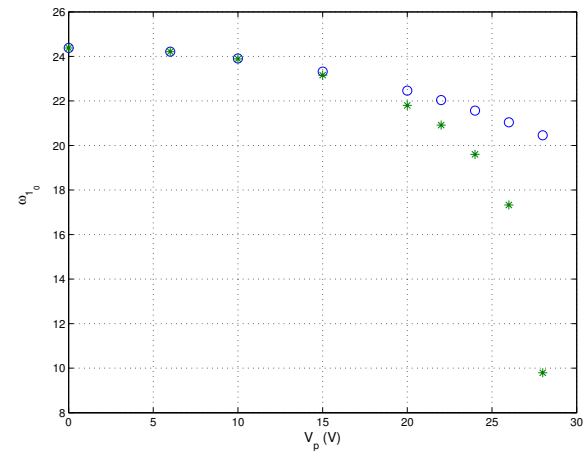
Figure 2: A comparison of the quality factors calculated using our model (circles) and the model in [3] (squares) with the experimental data (triangles) of Legtenberg and Tilmans [6].

In Figure 2, we show a comparison of the calculated quality factors for a microplate of lengths $310\mu\text{m}$ [6] using our model (circles) and a linear plate model [3] (squares), which neglects the in-plane displacements, with the experimental data (triangles) of Legtenberg and Tilmans [6]. The microbeam is actuated at $V_p = 2V$. We note that the model gives results very close to the model of Nayfeh and Younis [3] because the plate is actuated by a low DC voltage, in which the in-plane deflections are negligible. Therefore, we conclude that the simplified linear model in [3] produces accurate results at low DC loadings.

The operating conditions of many MEMS devices exceed the range of small DC loadings, such as in projection display arrays. In such cases, the in-plane displacements become significant, and hence a simple plate model that neglects the in-plane displacements as in [3] is suspect. In Figure 3, we show a comparison of the calculated quality factors and fundamental natural frequencies of a $210\mu\text{m}$ length microplate [6] using the



(a) Quality factors.



(b) Fundamental natural frequencies.

Figure 3: Variations of the quality factors and natural frequencies of a $210\mu\text{m}$ length microplate for various values of the DC voltage.

present model with those calculated using the simplified model in [3]. We note that the simplified model overestimates the quality factors and the natural frequencies at nearly 30% of the pull-in voltage. This is because, as the DC force increases, the static deflection increases, the gap width decreases, and hence the squeeze-film damping increases. Further, the increase in the electrostatic force decreases the natural frequencies. This effect is not represented correctly in the simplified model.

Figure 4 shows variation of the quality factor of the microplate of Figure 3 with V_p for various values of P_a . Clearly, the quality factor is a strong function of the gas pressure. Figure 5 shows the spatial variation of the pressure distribution P_{10} , corresponding to the first

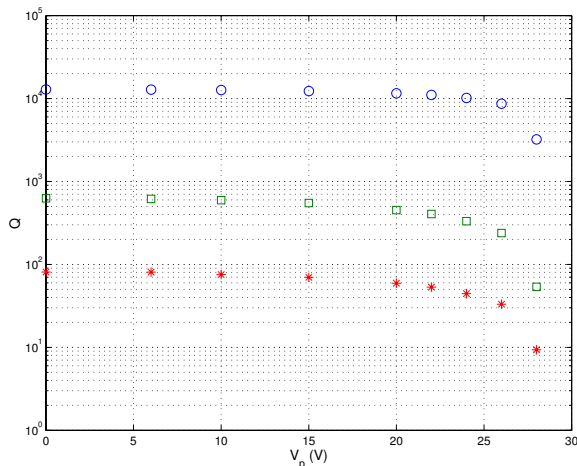


Figure 4: Variations of the quality factor with V_p for $P_a = .01mbar$ (circles), $P_a = 1mbar$ (squares), and $P_a = 10mbar$ (stars).

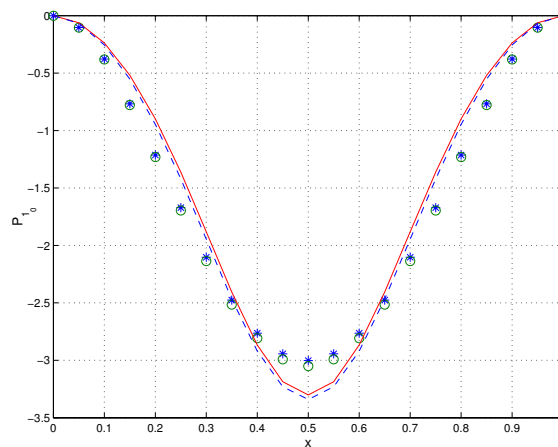
mode shape of the microplate of Figure 3, for various values of the electrostatic force and gap pressure. The function P_{1_0} is normalized such that its integral over the area of the plate is unity. We note that varying the pressure has a slight effect on P_{1_0} and that increasing the electrostatic loading has a much significant effect.

4 CONCLUSIONS

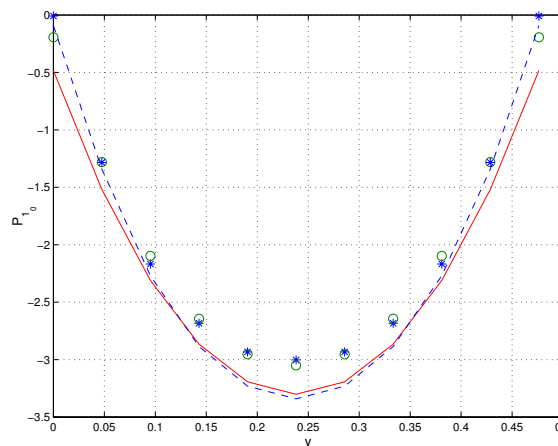
We presented a model for the dynamic behavior of microplates under the coupled effects of squeeze-film damping, electrostatic actuation, and mechanical forces. The model simulates the dynamics of microplates and predicts their quality factors under a wide range of gas pressures and applied electrostatic forces. The model presents a novel approach to the simulation of coupled-energy systems, which reduces the computational cost. The results show that the electrostatic force has more significant influence on the mechanical behavior of microplates than the encapsulation pressure. However, the pressure does affect the quality factor of microplates significantly.

REFERENCES

- [1] Yang, Y. J., Gretillat, M. A., and Senturia, S. D., "Effect of air damping on the dynamics of nonuniform deformations of microstructures," *Int. Conf. Solid State Sens. Actuat., TRANSDUCERS '97*, Chicago, Illinois, Vol. 2, 1997, pp. 1093–1096.
- [2] Younis, M. I., Abdel-Rahman, E. M., and Nayfeh, A. H., "A Reduced-order model for electrically actuated microbeam-based MEMS," *J. Microelectromech. Sys.*, Vol. 12, 2003, pp. 672–680.
- [3] Nayfeh, A. H. and Younis, M. I., "A new approach to the modeling and simulation of flexi-



(a) P_{1_0} at $y = b/2l$.



(b) P_{1_0} at $x = 1/2$.

Figure 5: The spatial variation of P_{1_0} when $V_p = 6V$ (discrete points) and $V_p = 28V$ (solid and dashes lines). The data shown in circles and dashed line corresponds to $P_a = 0.01mbar$ and the data in stars and solid line corresponds to $P_a = 2mbar$.

- ble microstructures under the effect of squeeze-film damping," *J. Micromech. Microeng.*, Vol. 14, 2004, pp. 170–181.
- [4] Veijola, T., Kuisma, H., Lahdenperä, J., and Ryhänen, T., "Equivalent-circuit model of the squeezed gas film in a silicon accelerometer," *Sens. Actuat. A*, Vol. 48, 1995, pp. 239–248.
- [5] Nayfeh, A. H., *Introduction to Perturbation Techniques*, Wiley, New York, 1981.
- [6] Legtenberg, R. and Tilmans, H. A., "Electrostatically driven vacuum-encapsulated polysilicon resonators. Part I. Design and fabrication," *Sens. Actuat. A*, Vol. 45, 1994, pp. 57–66.